Molecular structure and the twist-bend nematic phase: the role of terminal chains

Jordan P Abberley, Rebecca Walker, John MD Storey, and Corrie T Imrie*

Department of Chemistry, School of Natural and Computing Sciences, University of Aberdeen, Meston Building, Aberdeen AB24 3UE, UK

*Author for correspondence; email c.t.imrie@abdn.ac.uk

Abstract

The synthesis and characterisation of two homologous series of non-symmetric dimers are reported, the 1-(4-methoxybiphenyl-4'-yl)-6-(4-alkylanilinebenzylidene-4'-oxy)hexanes (MeOB6O.*m*, *m*=1-10) and 1-(4-methoxybiphenyl-4'-yl)-6-(4-alkyloxyanilinebenzylidene-4'-oxy)hexanes (MeOB6O.O*m*, *m*=1-9). All ten members of the MeOB6O.*m* series exhibit the conventional nematic phase. At lower temperatures the members with *m*=1-7 formed the twist-bend nematic phase, whereas for *m*=8-10 smectic behaviour replaced the twist-bend nematic, N_{TB}, phase. All nine members of the MeOB6O.O*m* also show the conventional nematic phase and for *m*=1-3, a strongly monotropic N_{TB} phase is also observed. The alkyloxy terminated dimers show the higher values of T_{NI} and $T_{N_{TB}N}$. For both series, the values of T_{NI} and $T_{N_{TB}N}$ show a modest alternation and in the same sense as *m* is increased. These observations suggest that the spatial uniformity of molecular curvature is important in driving the formation of the N_{TB} phase. The observation of smectic behaviour is attributed to the molecular inhomogeneity arising from the long terminal alkyl chain driving microphase separation. The transitional behaviour of these series is compared to those of the corresponding cyanobiphenyl-based series and overarching observations discussed.

1. Introduction

The discovery of the twist-bend nematic phase, N_{TB}, [1] and its subsequent verification [2, 3] triggered significant and global research interest. First predicted some thirty years earlier by Meyer [4] and later independently by Dozov [5], the N_{TB} phase is fascinating for a number of reasons but perhaps most so for the observation of spontaneous chirality in a collection of achiral molecules. Indeed, the N_{TB} phase provided the first example of spontaneous chiral symmetry breaking in a fluid with no spatial ordering. Dozov's prediction of the N_{TB} phase was underpinned by the assumption that bent molecules have a strong natural tendency to pack into bent structures [5]. However, pure uniform bend in space is not allowed, and must be accompanied by other local deformations of the director, namely, splay or twist. In the N_{TB} phase, the directors form a helix and are tilted with respect to the helical axis. The formation of this structural chirality is spontaneous, and so an equal number of the degenerate left- and right-handed helices would be expected. The introduction of intrinsic molecular chirality lifts this degeneracy and the chiral N_{TB} phase is observed [6].

The first assignment of the N_{TB} phase was for the liquid crystal dimer, CB7CB [1]:

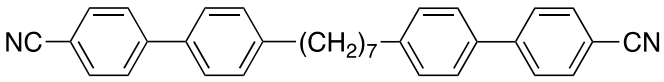

Liquid crystal dimers consist of molecules containing two mesogenic units connected *via* a flexible alkyl spacer, and their transitional behaviour is strongly dependent on the length and parity of the spacer [7-9]. This dependence is attributed to how the spacer controls the average molecular shape. Specifically, if an even number of atoms connect the two mesogenic units then the long axes of these moieties are essentially parallel, and the molecule is linear. By contrast, for an odd number of connecting atoms, the mesogenic groups are inclined at some angle with respect to each other, and the molecule is bent. Thus, CB7CB is, on average, a bent molecule, and the observation of the N_{TB} phase may be accounted for within the framework of Dozov's prediction [5]. Indeed, the vast majority of twist-bend nematogens may be described as odd-membered liquid crystal dimers (see for example [10-28]) although other structures including hydrogen-bonded materials [29-33], higher oligomers [34-40], polymers [41] and semi-rigid bent-core materials [42] have also been shown to exhibit the N_{TB} phase. In each of these classes of material, however, it is widely accepted that the stability of the N_{TB} phase is strongly dependent on molecular shape, and specifically, molecular curvature. This view is in accord with predictions made using a generalised Maier-Saupe theory for which the nematic-twist-bend nematic transition temperature is shown to be highly sensitive to the bend angle for V-shaped molecules [43, 44]. These bent materials have been shown to have considerable application potential [39, 45-47].

Dozov not only predicted that bent molecules may exhibit the N_{TB} phase but also that they may show heliconical smectic phases [5]. We recently reported the discovery of these twist-bend smectic phases for odd-membered liquid crystal dimers [48, 49]. In order to begin to establish the relationship between molecular structure and the formation of these new twist-bend phases, we investigated the transitional behaviour of two series of non-symmetric liquid crystal dimers in which the length of a terminal chain was varied, the 1-(4-cyanobiphenyl-4'-yl)-6-(4-alkyloxyanilinebenzylidene-4'-oxy)hexanes (CB6O.O*m*) [23],

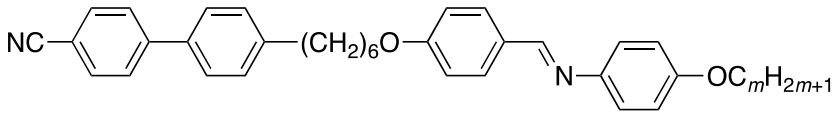

and the structurally similar 1-(4-cyanobiphenyl-4'-yl)-6-(4-alkylanilinebenzylidene-4'-oxy)hexanes (CB6O.*m*) [50],

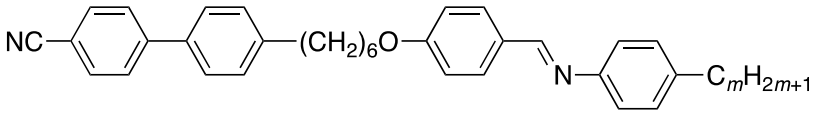

.

For the CB6O.O*m* series, N and N_{TB} phases were observed for all the homologues prepared (*m*=1-10) whereas smectic behaviour was seen only for *m*=3-5 [23]. All ten members of the CB6O.*m* (*m*=1-10) series also showed N and N_{TB} phases but only the decyl homologue exhibits smectic behaviour [49, 50]. To better understand the formation of smectic phases by bent non-symmetric dimers, we report here the synthesis and characterisation of the analogous materials but with a methoxy terminal substituent, the 1-(4-methoxybiphenyl-4'-yl)-6-(4-alkylanilinebenzylidene-4'-oxy)hexanes (MeOB6O.*m*), and 1-(4-methoxybiphenyl-4'-yl)-6-(4-alkyloxyanilinebenzylidene-4'-oxy)hexanes (MeOB6O.O*m*),

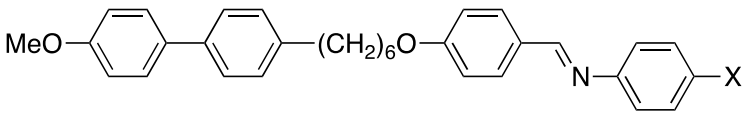

MeOB6O.*m* : X = C_mH_{2m+1} *m* = 1-10

MeOB6O.O*m* : X = OC_mH_{2m+1} *m* = 1-9

A comparison of the properties of these four series will allow us to comment on the importance of the polarity of the terminal group in stabilising the N_{TB} and smectic phases, and on the role played by the interaction between the unlike mesogenic groups in driving the formation of these phases.

2. Experimental

2.1. Materials

The synthetic routes used to obtain the MeOB6O.*m* and MeOB6O.O*m* series are shown in Scheme 1. Full synthetic descriptions and structural characterisation data for all the final products and their intermediates are given in the associated supplementary information.

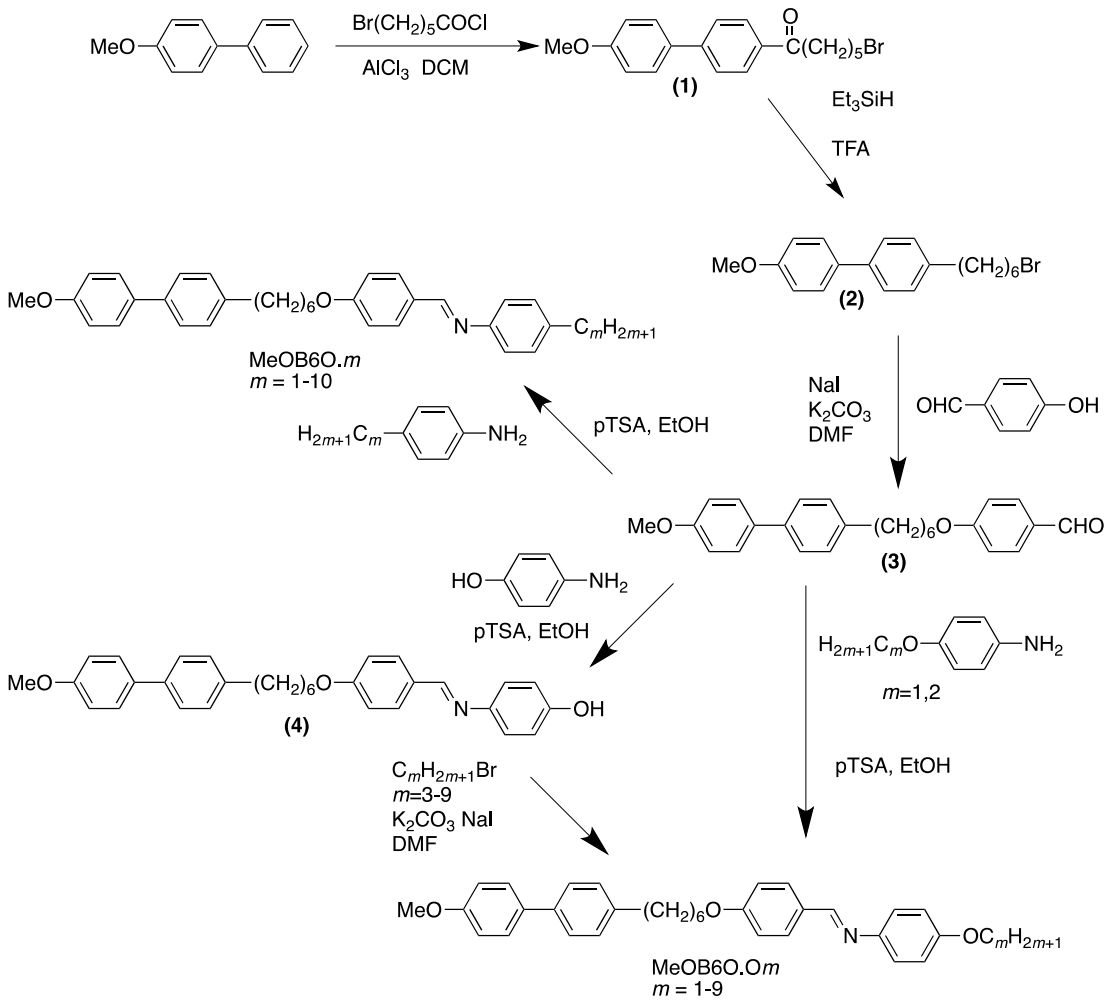

Scheme 1. The syntheses of the MeOB6O.*m* and MeOB6O.O*m* series.

2.2. Thermal characterisation

The phase behaviour of the compounds was studied by differential scanning calorimetry (DSC) using a Mettler-Toledo DSC820 fitted with an intracooler and calibrated using indium and zinc as standards. The thermograms were obtained during heating and cooling scans at 10ºC min^{-1}, under a nitrogen atmosphere. All samples were measured in duplicate. Transition temperatures and associated

enthalpy changes were extracted from the second-heating trace, and those listed are an average for both samples measured. Phase assignments were made by polarised optical microscopy (POM), using an Olympus BH2 microscope equipped with a Linkam TMHS 600 heating stage.

2.3 Molecular modelling

The geometric parameters and electronic properties of the dimers were calculated using quantum mechanical density functional theory [51]. Geometric optimisation of the dimers with the spacer in the all-*trans* conformation was performed using Gaussian G09W at the B3LYP/6–31G(d) level of theory. The all-*trans* conformers were selected for reasons discussed in detail elsewhere [10]. Visualisation of space-filling models of the output post-optimisation was performed using QuteMol [52] and Gaussview 5 was used for the visualisation of electrostatic potential isosurfaces, ball-and-stick models and dipole moments [53]

3. Results and Discussion

3.1. MeOB6O.m series

The transitional properties of the MeOB6O.*m* series are listed in Table 1. All ten members exhibit a conventional nematic (N) phase identified on the basis of the observation of characteristic optical textures when viewed through the polarised light microscope. Specifically, schlieren textures were seen containing both types of point singularities and which flashed when subjected to mechanical stress, see Figure 1(a). The scaled values of the entropy change associated with the N-isotropic (I) transition are listed in Table 1 and are wholly consistent with this assignment [54, 55]. On cooling isolated droplets of the N phase seen for the homologues with *m*=1-7, the schlieren texture changed to give regions of parabolic defects in coexistence with rope-like features, see Figure 1(b). In addition, the transition was accompanied by the cessation of optical flickering associated with the directors in the conventional N phase. In a cell treated for planar alignment, on cooling, the homogenous nematic texture changed to the characteristic striped texture of the N_{TB} phase, see Figure 2. On cooling the nematic phase seen for homologues with *m*=8-10, coexisting regions of focal conic fan and homeotropic textures developed suggesting the formation of a smectic A phase, see Figure 3. On further cooling, a schlieren texture containing two- and four-point brush defects developed from the homeotropically aligned regions, suggesting the formation of a tilted smectic phase (Figure 4). Two-brush defects are characteristic of phases in which the mesogenic units are arranged in an anticlinic fashion, suggesting this is the SmC_A phase. We cannot rule out the possibility, however, that this is an example of the heliconical SmC_{TB} phase having a distorted clock structure such that the molecular orientations are not fully averaged over the helix and for which a schlieren texture containing two-

and four-point brush defects may be observed [48, 49]. The monotropic nature of these smectic phases prevents their characterisation using resonant X-ray diffraction, and thus the assignment of the lower temperature phase as a SmC_A phase remans tentative.

Table 1. Transitional properties of the MeOB6O.*m* series. (Cr, Crystal; SmC, Smectic C; SmA, Smectic A; N_{TB}, Twist-Bend Nematic; N, Nematic; I, Isotropic.)

m	T_{CrI}/°C [a]T_{CrN}/°C	[†]T_{SmCSmA}/°C	[†]$T_{N_{TB}N}$/°C [†b]T_{SmAN}/°C	T_{NI}/°C	ΔH_{CrI} [a]ΔH_{CrN} / kJ mol^{-1}	ΔH_{NI} / kJ mol^{-1}	$\Delta S_{NI}/R$
1	129.6		79	119.8	54.58	0.82	0.25
2	119.5		68	109.7	47.34	0.52	0.16
3	[a]113.5		78	114.5	[a]46.02	0.61	0.19
4	111.8		69	106.3	46.41	0.42	0.13
5	113.1		78	110.3	46.44	0.47	0.15
6	111.4		65	101.2	49.44	*-	
7	111.7		78	105.5	47.19	*-	
8	110.4	82	[b]89	102.1	52.54	*-	
9	109.9	84	[b]87	102.2	50.23	0.55	0.18
10	108.6	87	[b]92	100.5	51.43	0.77	0.25

*Exotherms associated with crystallisation and the N-I transition overlap.

[†]Temperatures measured using the polarised light microscope on cooling.

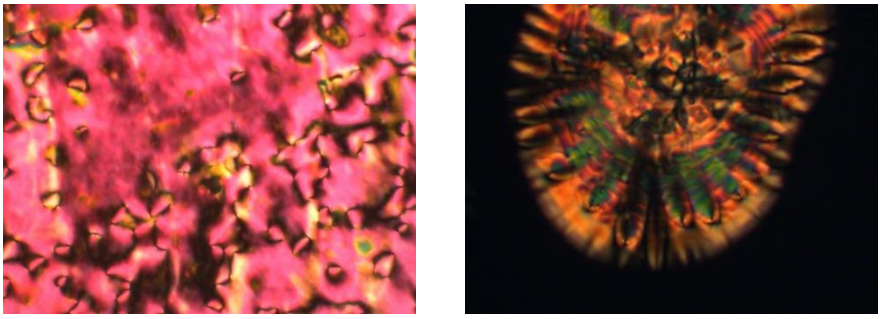

(a) (b)

Figure 1. (a) Nematic schlieren (T=102˚C) and (b) parabolic defect twist-bend nematic texture (T=75˚C) seen for MeOB6O.1.

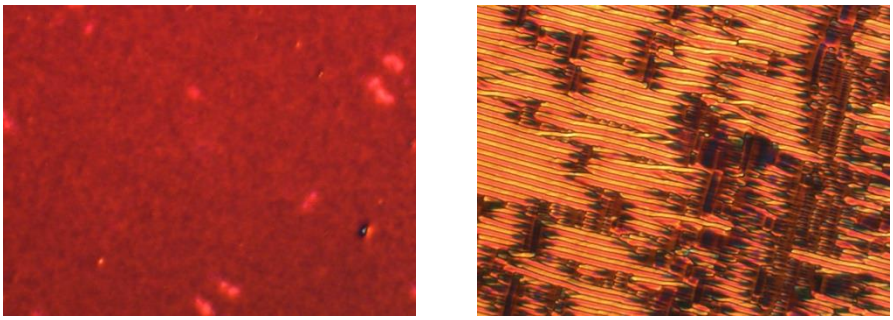

(a) (b)

Figure 2. (a) Homogeneous N texture (T=99˚C) and (b) striped N_{TB} texture (T=74˚C) observed for MeOB6O.1 in a 3 micron cell treated for planar alignment. The stripes are parallel to the rubbing direction.

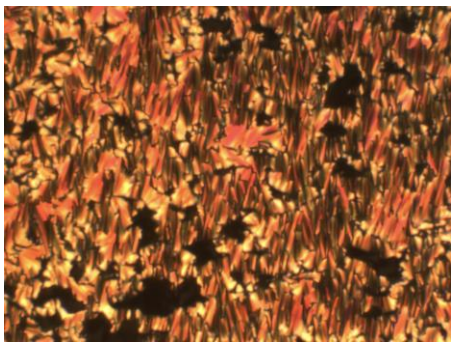

Figure 3. Focal conic fan texture in coexistence with regions of homeotropic alignment of the SmA phase seen for MeOB6O.10 at (T = 90 ˚C).

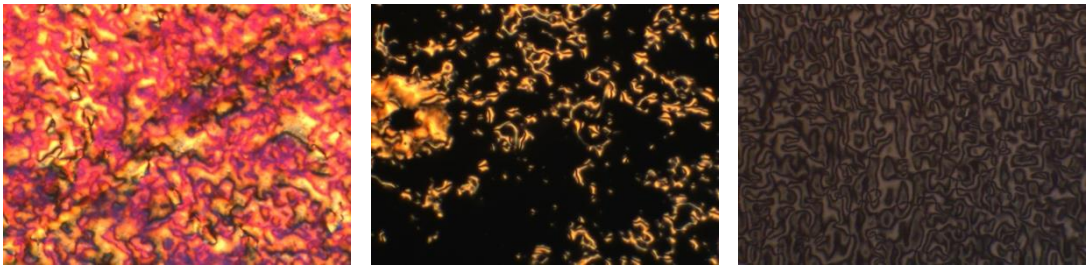

(a) (b) (c)

Figure 4. (a) Nematic schlieren texture (T=95˚C), (b) the predominantly homeotropically aligned smectic A phase (T=87˚C) and (c) the schlieren texture of the smectic C phase (T=78˚C) obtained on cooling MeOB6O.9.

In order to confirm that the smectic A phase observed for homologues with *m*=8-10 was not in fact the N_{TB} phase, a binary phase diagram was constructed for mixtures of MeOB6O.9 and the extensively studied twist bend nematogen, CB7CB [1], see Figure 5. The mixtures were prepared by codissolving preweighed amounts of the dimers in dichloromethane. The solvent was allowed to slowly evaporate at room temperature, and the mixture dried under vacuum at 50 °C overnight. All the mixtures exhibited the conventional nematic phase and complete miscibility of the nematic phase was observed for all compositions. Mixtures containing 36 mol % and greater CB7CB exhibited the N_{TB} phase, see Figure 6, whereas at lower concentrations SmA behaviour is seen and a discontinuity in the phase diagram is apparent. This confirms the smectic phase assignment on increasing *m*.

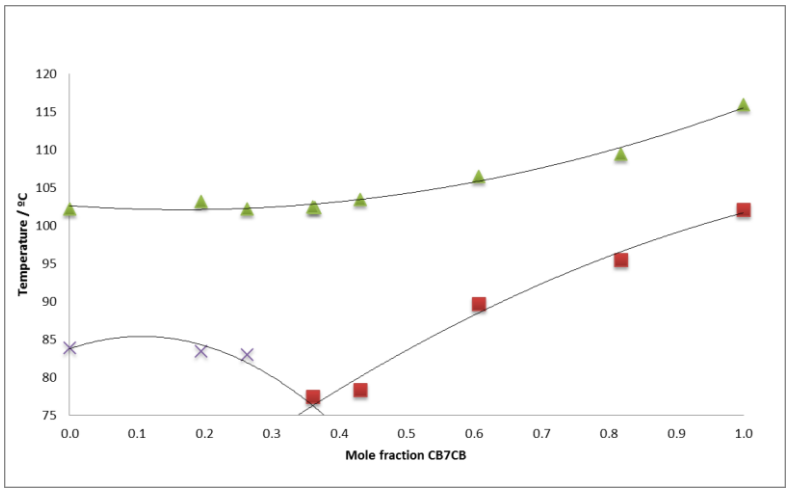

Figure 5. Phase diagram constructed for binary mixtures of MeOB6O.9 and CB7CB. Triangles represent N-I transitions, squares N_{TB}-N transitions and crosses SmA-N transitions. Melting points have been omitted for the sake of clarity.

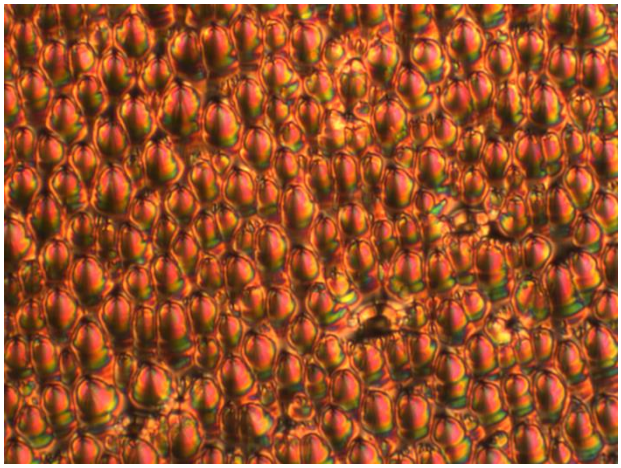

Figure 6. The polygonal texture seen for the N_{TB} phase of a binary mixture containing 64 mol% MeOB6O.9 and 36 mol% CB7CB (T = 72˚C).

The dependence of the transition temperatures on the length of the terminal alkyl chain, *m*, for the MeOB6O.*m* series is shown in Figure 7. It is immediately apparent that, with the exception of MeOB6O.3, the MeOB6O.*m* series are all monotropic nematogens. The melting point falls initially on increasing *m* but tends towards a limiting value as *m* increases further. The nematic-isotropic transition temperature, T_{NI}, tends to decrease on increasing *m* and superimposed on this is a modest alternation in which odd members show the higher values, and which attenuates on increasing *m*. This is characteristic behaviour for this class of material and may be attributed to the change in shape anisotropy on varying the parity of the terminal chain [56, 57]. Specifically, a methylene group added to an even-membered chain lies more or less parallel to the major molecular axis whereas if added to an odd-membered chain lies at an angle to this axis. Thus, a larger increase in the anisotropic shape of the molecule is evident on forming an odd-membered chain. The underlying decreasing trend in T_{NI} may be accounted for by the dilution of the interactions between the mesogenic units on increasing the length of the terminal chain. The rather small change in T_{NI} of less than 20 ˚C across the whole series is typical for a series of nematogens with values of T_{NI} slightly above about 100˚C [57]. For series showing higher values of T_{NI}, a more pronounced decrease is observed on increasing the terminal alkyl chain length arising from the dilution of the stronger interactions between the mesogenic units. By contrast, for nematogenic series with values of T_{NI} lower than about 100˚C, there is an underlying increase in T_{NI} on increasing chain length reflecting the enhanced molecular anisotropy associated with increasing the length of the chain. At around 100 ˚C these two effects are more or less balanced and a rather flat T_{NI} line is observed as seen in Figure 7. The twist-bend nematic-nematic transition temperature, $T_{N_{TB}N}$, also exhibits an alternation on increasing *m* and in the same sense as that seen for T_{NI}. Furthermore, $T_{N_{TB}N}$ does not show the same underlying decreasing trend as T_{NI} on increasing *m* such that increasing *m* stabilises the N_{TB} relative to the N phase. This

suggests that the effect of the terminal chain length on $T_{N_{TB}N}$ may also be accounted for in terms of the change in molecular shape anisotropy on varying *m*. It is interesting to note, however, that the values of $T_{N_{TB}N}$ for a given parity chain are rather insensitive to increases in chain length. This suggests that the dilution of the interactions between the cores arising from increasing chain length has a smaller effect on the predominantly shape driven N_{TB}-N transition than on the N-I transition. It may appear counter intuitive, therefore, that the sense of the alternation seen for $T_{N_{TB}N}$ and T_{NI} is the same given that molecular curvature is widely held to be a prerequisite for the observation of the N_{TB} phase. Thus, increasing the molecular shape anisotropy increasing T_{NI} might be expected to reduce $T_{N_{TB}N}$ and *vice versa*, so giving an alternation in the opposite sense. It has been shown, however, that for liquid crystal dimers a spatially uniform molecular curvature is required to promote the N_{TB} phase such that the photoisomerization of a twist-bend azobenzene-based nematogen to the bent *cis* isomer destroys the N_{TB} phase [58]. Similar observations have been made for the dependence of $T_{N_{TB}N}$ and T_{NI} for other liquid crystal dimer series [23, 50]. This suggests that odd-membered chains which greater enhance the anisometric shape of the molecule also maintain the spatial uniformity of the molecular curvature. Smectic behaviour emerges for the longest three members of the MeOB6O.*m* series and the N_{TB} phase is extinguished. The emergence of smectic behaviour for long terminal chains is in accord with the general observation that for smectic phases to be observed in symmetric or non-symmetric dimers in which the mesogenic units do not show a specific favourable interaction, the combined lengths of the terminal chains has to exceed that of the flexible spacer [56, 59]. It has been suggested that the interaction between the terminal chains and spacer is an unfavourable one and must be offset by a specific favourable interaction between the unlike mesogenic units. If present, such an interaction drives the formation of an intercalated phase providing the combined lengths of the terminal chain is less than or comparable to the spacer length [60, 61]. Otherwise, a monolayer smectic phase is observed providing the combined length of the terminal chains exceeds that of the spacer, driven by the increased molecular inhomogeneity arising from the long terminal alkyl chain.

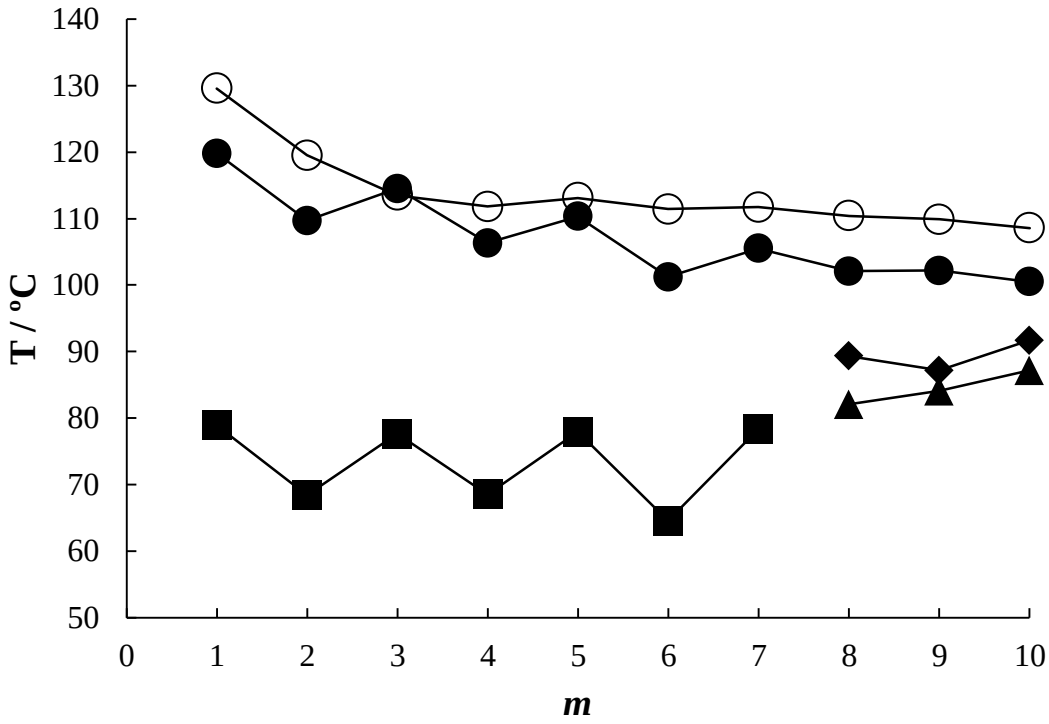

Figure 7. The dependence of the transition temperatures on the number of carbon atoms, *m*, in the terminal alkyl chain for the MeOB6O.*m* series. Empty circles indicate melting points, filled circles nematic-isotropic transition temperatures, filled squares twist-bend nematic-nematic transitions, filled diamonds smectic A-nematic transitions and filled triangles smectic C-smectic A transitions.

The transitional properties of the MeOB6O.O*m* series are listed in Table 2. All nine members exhibit a monotropic, conventional nematic phase. In addition, for *m*=1-3 a strongly monotropic N_{TB} phase is observed. Phases assignments were based on the observation of characteristic optical textures as described earlier. The dependence of the transition temperatures on the length of the terminal alkyl chain length *m* is shown in Figure 8, and it is apparent that the behaviour observed is similar to that seen in Figure 7 for the MeOB6O.*m* series. The larger decrease in T_{NI} across the series may be attributed to the higher interaction strength parameters between the mesogenic units which is reflected in the higher values of T_{NI}, and the more significant role of the chain in diluting these. We note that even members of this series now show the higher values of T_{NI} and $T_{N_{TB}N}$ because the oxygen atom must be considered part of the chain, and hence an even-membered carbon chain corresponds to an overall odd membered chain. The absence of either N_{TB} or smectic behaviour on increasing *m* for the MeOB6O.O*m* series may be attributed to the higher melting points of this series and the difficulty associated with supercooling the monotropic nematic phases.

Table 2. Transitional properties of the MeOB6O.O*m* series. (Cr, Crystal; N_{TB}, Twist-Bend Nematic; N, Nematic; I, Isotropic.)

m	T_{CrI}/°C	$^{\dagger}T_{N_{TB}N}$/°C	T_{NI}/°C	ΔH_{CrI} / kJ mol^{-1}	ΔH_{NI} / kJ mol^{-1}	$\Delta S_{NI}/R$
1	154.8	98	147.8	60.76	0.79	0.23
2	152.1	106	151.4	57.27	0.86	0.24
3	153.2	91	136.1	56.98	0.45	0.13
4	149.7		139.3	59.43	0.45	0.13
5	146.9		129.7	61.31	0.48	0.14
6	144.9		129.6	63.99	-	*-
7	143.8		125.1	56.82	0.47	0.14
8	142.5		125.3	64.98	0.56	0.17
9	141.5		123.4	67.11	-	*-

*Exotherms associated with crystallisation obscured that associated with the N-I transition.

†Temperatures measured using the polarised light microscope on cooling.

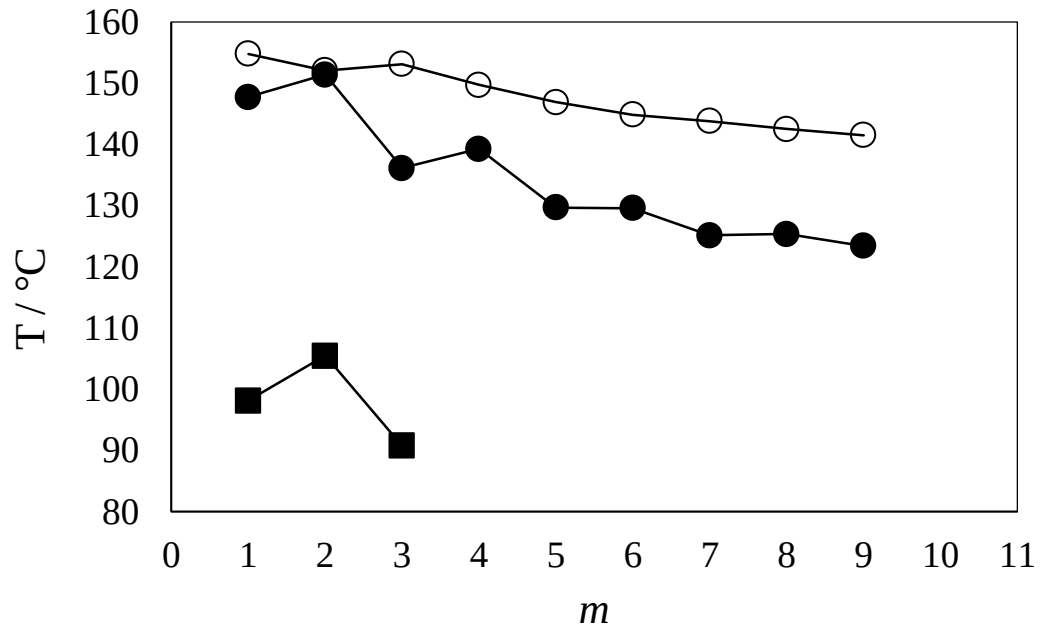

Figure 8. The dependence of the transition temperatures on the number of carbon atoms, *m*, in the terminal alkyl chain the MeOB6O.O*m* series. ◯ indicates melting points, nematic-isotropic transition temperatures, and twist-bend nematic-nematic transitions.

The melting points of the four series, MeOB6O.*m*, MeOB6O.O*m*, CB6O.*m*, and CB6O.O*m*, are compared in Figure 9. The MeOB6O.O*m* series shows the highest melting points for all values of *m*. The melting points of the MeOB6O.*m* dimers are higher than the corresponding members of the CB6O.*m* series except for the propyl homologues for which CB6O.3 has a marginally higher melting point than MeOB6O.3. For shorter terminal chains, the CB6O.O*m* dimers show the second highest melting points but these fall quickly as *m* is increased and for the higher values of *m* the melting points of the corresponding members of the CB6O.*m*, and CB6O.O*m* series are very similar and lower than those of the MeOB6O.*m* series. These data support the general observation that the methoxy group promotes higher melting points than a nitrile terminal group [62-64], and dimers having terminal alkoxy chains have higher melting points than the corresponding alkyl substituted materials [23, 50]. These trends may be attributed to the more efficient packing of the methoxy group and alkoxy chains compared to the nitrile and alkyl chains, respectively, and the enhanced polar interactions between alkoxy chains.

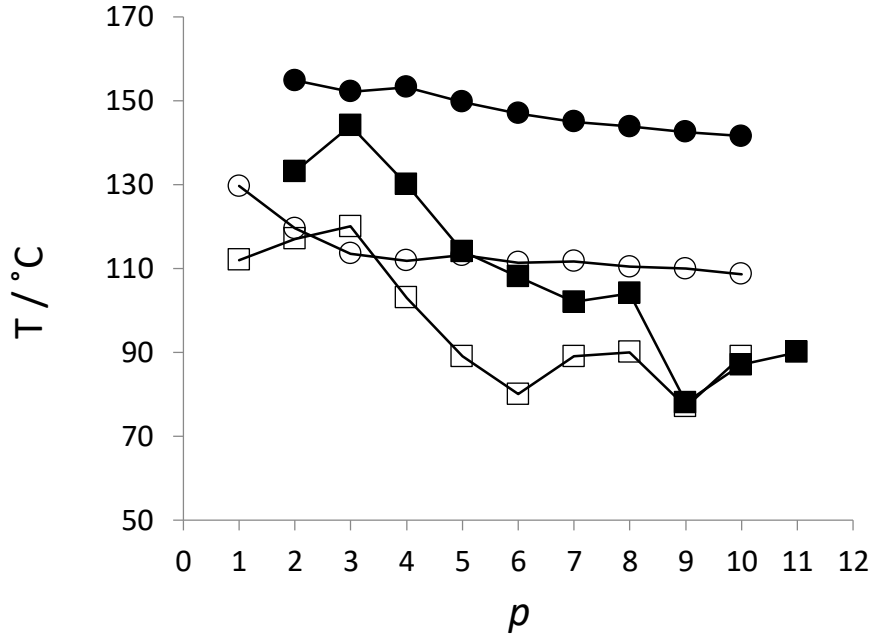

Figure 9. A comparison of the melting points as a function of the length of the terminal chain, *p*, for the MeOB6O.O*m* (filled circles), MeOB6O.*m* (empty circles), CB6O.O*m* (filled squares), and CB6O.*m* (empty squares) series. For the MeOB6O.*m* and CB6O.*m* series, *p*=*m* and for the MeOB6O.O*m* and CB6O.O*m* series, *p*=*m*+1.

The nematic-isotropic transition temperatures, T_{NI}, of the MeOB6O.O*m* and MeOB6O.*m* series are compared in Figure 10. The value of T_{NI} for a given member of the MeOB6O.O*m* series is higher than that of the corresponding member of the MeOB6O.*m* series. These differences are greater for shorter chains; for example, T_{NI} for MeOB6O.O1 is 38.1 ˚C higher than that of MeOB6O.2 whereas for the highest three values of *m* this difference has fallen to around 23 ˚C. The values of T_{NI} for the CB6O.O*m* and CB6O.*m* series are also shown on Figure 10 and similar behaviour is observed such that T_{NI} for a given member of the CB6O.O*m* series is higher than that of the corresponding member of the CB6O.*m* series. The differences in T_{NI} are also similar; for example, T_{NI} for CB6O.O1 is 35 ˚C higher than that of CB6O.2, and this difference falls to 25 ˚C when comparing the values of T_{NI} for CB6O.O9 and CB6O.10. The increase in T_{NI} on changing an alkyl to an alkyloxy chain may be attributed to the associated change in the average molecular shape. An alkyloxy chain lies more or less in the plane of the ring to which it is attached whereas an alkyl chain protrudes at an angle, see Figure 11. The greater shape anisotropy of the former accounts for the observed higher values of T_{NI}. On increasing chain length, conformational averaging reduces this difference in shape and the differences in T_{NI} between the corresponding alkyloxy and alkyl series become smaller. It is apparent that the cyanobiphenyl-based series show higher values of T_{NI} than their methoxybiphenyl-based counterparts. For smaller values of *m* this difference is around 10 ˚C and falls to essentially 0 ˚C as *m*

is increased. This may be accounted for in terms of the change of shape arising from exchanging a nitrile for a methoxy group [10] and the tendency of cyanobiphenyl units to arrange themselves in an anti-parallel fashion so enhancing structural anisotropy [65]. The convergence of the values of T_{NI} for the two alkyloxy and alkyl series as the length of the terminal chain increases, suggests that the difference in shape may be the more significant of these contributions given that this is reduced as the molecules become larger.

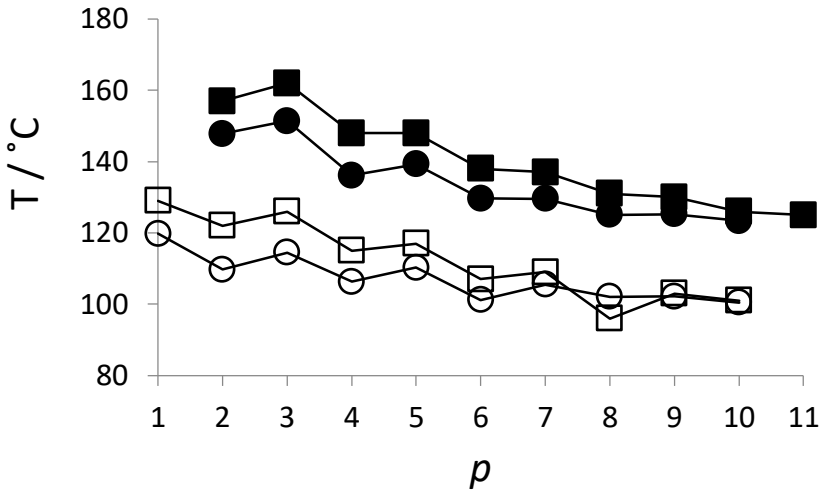

Figure 10. A comparison of the dependence of the nematic-isotropic transition temperatures, T_{NI}, on the length of the terminal chain *p* for the MeOB6O.*m* (empty circles), MeOB6O.O*m* (filled circles), CB6O.*m* (empty squares) and CB6O.O*m* (filled squares) series. For the alkyl series $p = m$ and for the alkoxy series $p = m+1$.

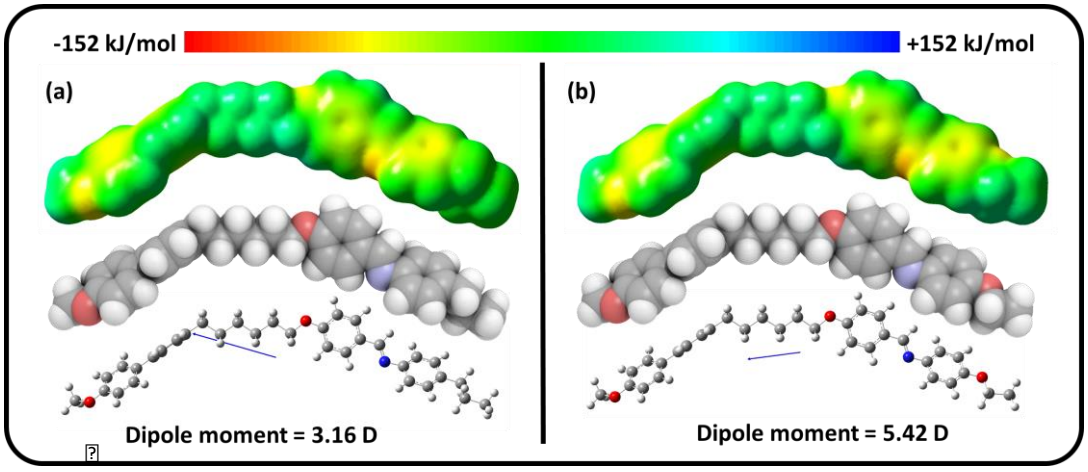

Figure 11. The electrostatic potential isosurfaces (top), space filling (middle) and ball-and-stick models showing the molecular dipole moment (not to scale, bottom) of (a) MeOB6O.3 and (b) MeOB6O.O2.

Figure 12 compares the dependence of the twist-bend nematic – nematic transition temperature, $T_{N_{TB}N}$, on the length of the terminal chain for the four series. Rather similar behaviour is seen as for T_{NI} in Figure 10. For both sets of dimers, the alkyloxy series shows the higher values of $T_{N_{TB}N}$ although the differences are smaller at around 10 ˚C and decrease with increasing *m*. Presumably a similar argument holds as described for the effects on T_{NI}, and that the alkyloxy chain allows for a more spatially uniform molecular curvature facilitating the local packing of these bent molecules. Changing the terminal substituent from a nitrile to a methoxy group also effects $T_{N_{TB}N}$ in a similar fashion to T_{NI}. Thus, for short terminal chains a reduction in $T_{N_{TB}N}$ of around 10 ˚C is observed and this difference becomes smaller as *m* is increased. Again, this suggests that the shapes of these dimers become more similar as *m* is increased, and that the molecular curvature is determined largely by the hexyloxy spacer. Molecular curvature plays a major role in determining the bend elastic constant that drives the formation of the N_{TB} phase [66]. The difference in N_{TB} between these particular series may be attributed, at least in part, to a specific favourable interaction between the cyanobiphenyl and benzylideneaniline moieties which is thought to play an important role in determining the phase behaviour of oligomers containing these units [23, 50, 67, 68]. The nature of this interaction is unclear but has been suggested to be an electrostatic quadrupolar interaction between fragments having quadrupoles of opposite signs [69]. It is clear that the electron distributions in the differing mesogenic units for the MeOB6O.O*m* and MeOB6O.*m* series are rather similar and a specific favourable interaction between would not be expected, although we note that the dipole moments of these systems are rather different see Figure 11. For the CB6O.O*m* and CB6O.*m* series the specific favourable interaction between the unlike mesogenic groups presumably provides an additional force for the formation of both the N_{TB} and N phases.

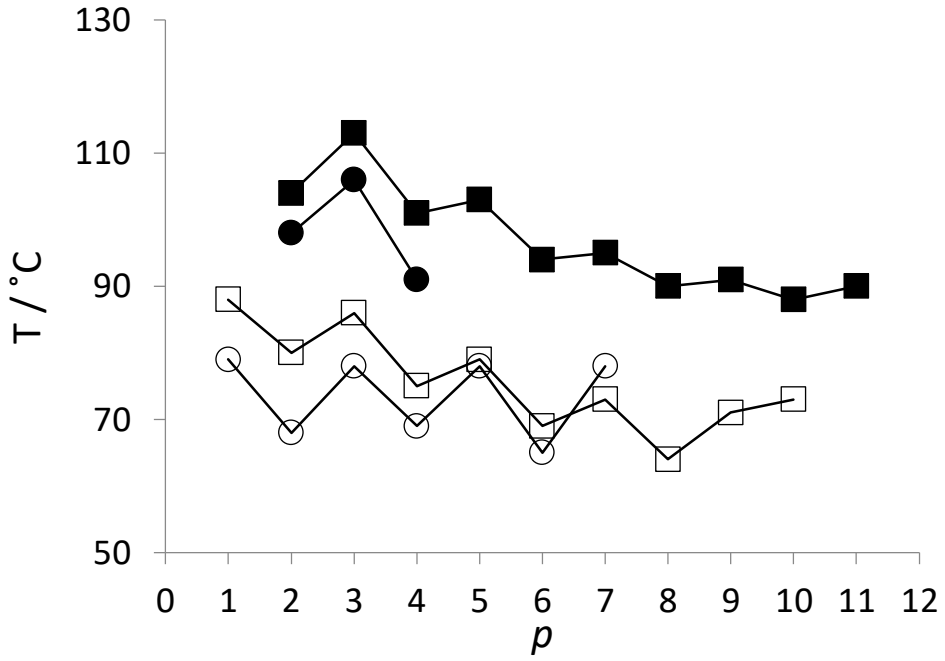

Figure 12. A comparison of the dependence of the twist-bend nematic-nematic transition temperatures, $T_{N_{TB}N}$, on the length of the terminal chain *p* for the MeOB6O.*m* (empty circles), MeOB6O.O*m* (filled circles), CB6O.*m* (empty squares) and CB6O.O*m* (filled squares) series. For the alkyl series $p = m$ and for the alkoxy series $p = m+1$.

Figure 13 compares the scaled entropies of transition associated with the nematic-isotropic transition, $\Delta S_{NI}/R$, on the length of the terminal chain for all four series. All the values are small and consistent with those expected for an odd-membered liquid crystal dimer [70]. The differences between the values are rather small when compared to experimental error although it appears that the cyanobiphenyl-based series tend to show slightly higher values and this reinforces the view that the nitrile group enhances the structural anisotropy of these materials [71, 72].

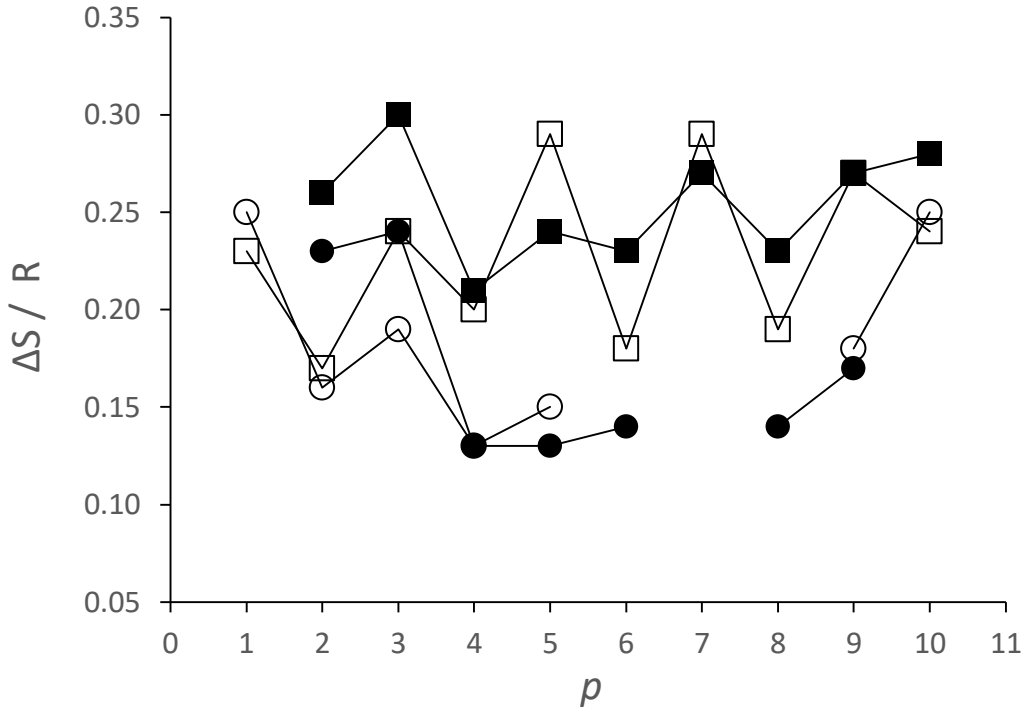

Figure 13. A comparison of the scaled entropy of transition associated with the nematic-isotopic transition, $\Delta S_{NI}/R$, on the length of the terminal chain *p* for the MeOB6O.*m* (empty circles), MeOB6O.O*m* (filled circles), CB6O.*m* (empty squares) and CB6O.O*m* (filled squares) series. For the alkyl series $p = m$ and for the alkoxy series $p = m+1$.

Of the four series of dimers discussed in this paper, all thirty-nine dimers exhibit nematic behaviour but just seven show smectic phases. This reflects the difficulties that bent odd-membered dimers experience in packing into smectic layered arrangements [56, 60, 61]. An intercalated SmC_A [23] or SmC_{TB} [49] phase is observed in the CB6O.O*m* series for *m*=3-5 whereas at the same temperature, the corresponding CB6O.*m* homologues show a nematic phase, and the MeOB6O.*m* dimers either nematic or twist-bend nematic behaviour. The enhanced tendency for the CB6O.O*m* to exhibit intercalated smectic behaviour may be attributed to an enhanced favourable specific interaction between the unlike mesogenic units [73]. These phases are only observed for intermediate chain lengths in the series because the terminal chain must be accommodated in the space defined by the length of the spacer. The absence of smectic behaviour for the CB6O.*m* dimers reflects the relative difficulty in packing the alkyl chains which, as we saw earlier, protrude at some angle from the benzylideneaniline units into such an intercalated structure, whereas for the methoxybiphenyl-based dimers there is no specific interaction between the unlike mesogenic units to drive the formation of an

intercalated arrangement. The three longest members of the MeOB6O.*m* series exhibit a SmA phase whereas at the same temperature nematic or twist-bend nematic behaviour is seen for the corresponding homologues of the CB6O.O*m* and CB6O.*m* series. The monotropic nature of the smectic phases shown by these compounds precludes their study using X-ray diffraction but likely to have a monolayer arrangement [59]. The only direct comparison that is possible is between the transition temperatures of MeOB6O.10 and CB6O.10. The values of T_{NI} are essentially identical whereas MeOB6O.10 shows SmC-SmA and SmA-N transitions at 78 and 92 ˚C, respectively, and CB6O.10 a Sm-N_{TB} and N_{TB}N transitions at 67 and 73 ˚C, respectively. The stronger tendency of MeOB6O.10 to exhibit smectic behaviour suggests that the increased molecular inhomogeneity promotes microphase separation driving the formation of a smectic phase. For CB6O.10 for which the molecular inhomogeneity would appear very similar, microphase separation is counteracted by the specific favourable interaction between the unlike mesogenic units that promotes mixing. Furthermore, the decyl terminal chain is too long to be accommodated within an intercalated smectic structure and hence nematic behaviour is observed to lower temperatures.

4. Conclusions

The transitional properties of the MeOB6O.*m* and MeOB6O.O*m* series are broadly similar to those of the very few series already reported in the literature that exhibit the twist-bend nematic phase, and in which a terminal chain is varied in length. The data reported here allow us to begin to discuss what appear to be general patterns of behaviour. Thus, for both series the values of T_{NI} and $T_{N_{TB}N}$ show a modest alternation and in the same sense on increasing *m*. This counter-intuitive observation suggests that the spatial uniformity of molecular curvature is important in driving the formation of the N_{TB} phase. Furthermore, increasing the terminal chain length, increases the ratio $T_{N_{TB}N}$/ T_{NI} suggesting that the dilution of the interactions between the mesogenic units arising from increasing chain length has a relatively smaller effect on the predominantly shape driven N_{TB}-N transition than on the N-I transition. In addition, dimers with alkyloxy terminal chains show higher values of both T_{NI} and $T_{N_{TB}N}$ than the corresponding alkyl substituted materials, and this may be attributed to the relative disposition of the chain with respect to the mesogenic moiety to which it is attached. These differences in transition temperatures become smaller as the chain length is increased. Again, this supports the view that the spatial uniformity of molecular curvature is important. Replacing a nitrile by a methoxy terminal group reduces both T_{NI} and $T_{N_{TB}N}$, and again these reductions are smaller as the chain length is extended suggesting that they are associated with a change in molecular shape which is diluted as the molecule becomes larger. In these particular sets of materials the differences in transitional behaviour may be also be attributed, in part, to the specific favourable interaction between the cyanobiphenyl and benzylideneaniline moieties which are not present in the methoxybiphenyl-

based dimers. This is particularly true when considering the occurrence of smectic behaviour. The thirty-nine dimers discussed here are all predominantly nematogens and this reflects the difficulty bent dimers experience in packing into layered smectic arrangements. Intermediate members of the CB6O.O*m* series exhibit an intercalated smectic phase driven by the interaction between the unlike mesogenic groups. By comparison, the longest members of the MeOB6O.*m* series shown an enhanced tendency to exhibit smectic behaviour attributed to the molecular inhomogeneity arising from the long terminal chain.

References

1. Cestari M, Diez-Berart S, Dunmur DA, Ferrarini A, de la Fuente MR, Jackson DJB, Lopez DO, Luckhurst GR, Perez-Jubindo MA, Richardson RM, Salud J, Timimi BA, Zimmermann H. Phase behavior and properties of the liquid-crystal dimer 1 ",7 "-bis(4-cyanobiphenyl-4 '- yl) heptane: A twist-bend nematic liquid crystal. Phys Rev E. 2011;84:031704.
2. Borshch V, Kim YK, Xiang J, Gao M, Jakli A, Panov VP, Vij JK, Imrie CT, Tamba MG, Mehl GH, Lavrentovich OD. Nematic twist-bend phase with nanoscale modulation of molecular orientation. Nat Commun. 2013;4:2635.
3. Zhu CH, Tuchband MR, Young A, Shuai M, Scarbrough A, Walba DM, Maclennan JE, Wang C, Hexemer A, Clark NA. Resonant Carbon K-Edge Soft X-Ray Scattering from Lattice-Free Heliconical Molecular Ordering: Soft Dilative Elasticity of the Twist-Bend Liquid Crystal Phase. Phys Rev Lett. 2016;116:147803.
4. Meyer RB. Structural problems in liquid crystal physics, Les houches summer school in theoretical physics. In: Balian R, Weil G, editors. Molecular Fluids New York: Gordon and Breach; 1976. p. 273-373.
5. Dozov I. On the spontaneous symmetry breaking in the mesophases of achiral banana-shaped molecules. Europhys Lett. 2001;56:247-53.
6. Walker R, Pociecha D, Storey JMD, Gorecka E, Imrie CT. The Chiral Twist-Bend Nematic Phase (N*(TB)). Chem Eur J. 2019;25:13329-35.
7. Imrie CT, Henderson PA. Liquid crystal dimers and oligomers. Curr Opin Colloid Interface Sci. 2002;7:298-311.
8. Imrie CT, Henderson PA. Liquid crystal dimers and higher oligomers: Between monomers and polymers. Chem Soc Rev. 2007;36:2096-124.
9. Imrie CT, Henderson PA, Yeap G-Y. Liquid crystal oligomers: going beyond dimers. Liq Cryst. 2009;36:755-77.

10. Abberley JP, Jansze SM, Walker R, Paterson DA, Henderson PA, Marcelis ATM, Storey JMD, Imrie CT. Structure-property relationships in twist-bend nematogens: the influence of terminal groups. Liq Cryst. 2017;44:68-83.
11. Paterson DA, Walker R, Abberley JP, Forestier J, Harrison WTA, Storey JMD, Pociecha D, Gorecka E, Imrie CT. Azobenzene-based liquid crystal dimers and the twist-bend nematic phase. Liq Cryst. 2017;44:2060-78.
12. Paterson DA, Abberley JP, Harrison WT, Storey JM, Imrie CT. Cyanobiphenyl-based liquid crystal dimers and the twist-bend nematic phase. Liq Cryst. 2017;44:127-46.
13. Archbold CT, Andrews JL, Mandle RJ, Cowling SJ, Goodby JW. Effect of the linking unit on the twist-bend nematic phase in liquid crystal dimers: a comparative study of two homologous series of methylene- and ether-linked dimers. Liq Cryst. 2017;44:84-92.
14. Mandle RJ, Voll CCA, Lewis DJ, Goodby JW. Etheric bimesogens and the twist-bend nematic phase. Liq Cryst. 2016;43:13-21.
15. Mandle RJ, Davis EJ, Voll CCA, Archbold CT, Goodby JW, Cowling SJ. The relationship between molecular structure and the incidence of the N-TB phase. Liq Cryst. 2015;42:688-703.
16. Lu ZB, Henderson PA, Paterson BJA, Imrie CT. Liquid crystal dimers and the twist-bend nematic phase. The preparation and characterisation of the alpha,omega-bis(4-cyanobiphenyl-4 '-yl) alkanedioates. Liq Cryst. 2014;41:471-83.
17. Cruickshank E, Salamonczyk M, Pociecha D, Strachan GJ, Storey JMD, Wang C, Feng J, Zhu CH, Gorecka E, Imrie CT. Sulfur-linked cyanobiphenyl-based liquid crystal dimers and the twist-bend nematic phase. Liq Cryst. 2019;46:1595-609.
18. Dawood AA, Grossel MC, Luckhurst GR, Richardson RM, Timimi BA, Wells NJ, Yousif YZ. Twist-bend nematics, liquid crystal dimers, structure-property relations. Liq Cryst. 2017;44:106-26.
19. Dawood AA, Grossel MC, Luckhurst GR, Richardson RM, Timimi BA, Wells NJ, Yousif YZ. On the twist-bend nematic phase formed directly from the isotropic phase. Liq Cryst. 2016;43:2-12.
20. Arakawa Y, Komatsu K, Tsuji H. Twist-bend nematic liquid crystals based on thioether linkage. New J Chem. 2019;43:6786-93.
21. Henderson PA, Imrie CT. Methylene-linked liquid crystal dimers and the twist-bend nematic phase. Liq Cryst. 2011;38:1407-14.
22. Abberley JP, Storey JMD, Imrie CT. Structure-property relationships in azobenzene-based twist-bend nematogens. Liq Cryst. 2019;46:2102-14.
23. Paterson DA, Crawford CA, Pociecha D, Walker R, Storey JMD, Gorecka E, Imrie CT. The role of a terminal chain in promoting the twist-bend nematic phase: the synthesis and characterisation of the 1-(4-cyanobiphenyl-4'-yl)-6-(4-alkyloxyanilinebenzylidene-4'-oxy)hexanes. Liq Cryst. 2018;45:2341-51.

24. Paterson DA, Gao M, Kim YK, Jamali A, Finley KL, Robles-Hernandez B, Diez-Berart S, Salud J, de la Fuente MR, Timimi BA, Zimmermann H, Greco C, Ferrarini A, Storey JMD, Lopez DO, Lavrentovich OD, Luckhurst GR, Imrie CT. Understanding the twist-bend nematic phase: the characterisation of 1-(4-cyanobiphenyl-4 '-yloxy)-6-(4-cyanobiphenyl-4 '-yl)hexane (CB6OCB) and comparison with CB7CB. Soft Matter. 2016;12:6827-40.
25. Ramou E, Welch C, Hussey J, Ahmed Z, Karahaliou PK, Mehl GH. The induction of the N-tb phase in mixtures. Liq Cryst. 2018;45:1929-35.
26. Lesac A, Baumeister U, Dokli I, Hamersak Z, Ivsic T, Kontrec D, Viskic M, Knezevic A, Mandle RJ. Geometric aspects influencing N-N-TB transition - implication of intramolecular torsion. Liq Cryst. 2018;45:1101-10.
27. Watanabe K, Tamura T, Kang SM, Tokita M. Twist bend nematic liquid crystals prepared by one-step condensation of 4-(4-Pentylcyclohexyl) benzoic acid and alkyl diol. Liq Cryst. 2018;45:924-30.
28. Arakawa Y, Tsuji H. Selenium-linked liquid crystal dimers for twist-bend nematogens. J Molec Liq. 2019;289:111097.
29. Paterson DA, Martinez-Felipe A, Jansze SM, Marcelis ATM, Storey JMD, Imrie CT. New insights into the liquid crystal behaviour of hydrogen-bonded mixtures provided by temperature-dependent FTIR spectroscopy. Liq Cryst. 2015;42:928-39.
30. Jansze SM, Martinez-Felipe A, Storey JMD, Marcelis ATM, Imrie CT. A Twist-Bend Nematic Phase Driven by Hydrogen Bonding. Angew Chem Int Ed. 2015;54:643-6.
31. Walker R, Pociecha D, Martinez-Felipe A, Storey JMD, Gorecka E, Imrie CT. Twist-Bend Nematogenic Supramolecular Dimers and Trimers Formed by Hydrogen Bonding. Crystals. 2020;10:175.
32. Walker R, Pociecha D, Crawford CA, Storey JMD, Gorecka E, Imrie CT. Hydrogen bonding and the design of twist-bend nematogens. J Molec Liq. 2020;303:112630.
33. Walker R, Pociecha D, Abberley JP, Martinez-Felipe A, Paterson DA, Forsyth E, Lawrence GB, Henderson PA, Storey JMD, Gorecka E, Imrie CT. Spontaneous chirality through mixing achiral components: a twist-bend nematic phase driven by hydrogen-bonding between unlike components. Chem Commun. 2018;54:3383-6.
34. Mandle RJ, Goodby JW. A Nanohelicoidal Nematic Liquid Crystal Formed by a Non-Linear Duplexed Hexamer. Angew Chem Int Ed. 2018;57:7096-100.
35. Simpson FP, Mandle RJ, Moore JN, Goodby JW. Investigating the Cusp between the nano- and macro-sciences in supermolecular liquid-crystalline twist-bend nematogens. J Mater Chem C. 2017;5:5102-10.
36. Mandle RJ, Goodby JW. A Liquid Crystalline Oligomer Exhibiting Nematic and Twist-Bend Nematic Mesophases. Chem Phys Chem. 2016;17:967-70.

37. Tuchband MR, Paterson DA, Salamonczykc M, Norman VA, Scarbrough AN, Forsyth E, Garcia E, Wang C, Storey JMD, Walba DM, Sprunt S, Jakli A, Zhu CH, Imrie CT, Clark NA. Distinct differences in the nanoscale behaviors of the twist-bend liquid crystal phase of a flexible linear trimer and homologous dimer. Proc Natl Acad Sci U S A. 2019;116:10698-704.
38. Wang Y, Singh G, Agra-Kooijman DM, Gao M, Bisoyi HK, Xue CM, Fisch MR, Kumar S, Li Q. Room temperature heliconical twist-bend nematic liquid crystal. Crystengcomm. 2015;17:2778-82.
39. Wang Y, Zheng ZG, Bisoyi HK, Gutierrez-Cuevas KG, Wang L, Zola RS, Li Q. Thermally reversible full color selective reflection in a self-organized helical superstructure enabled by a bent-core oligomesogen exhibiting a twist-bend nematic phase. Mater Horizons. 2016;3:442-6.
40. Arakawa Y, Komatsu K, Inui S, Tsuji H. Thioether-linked liquid crystal dimers and trimers: The twist-bend nematic phase. J Molec Str. 2020;1199:126913.
41. Stevenson WD, An JG, Zeng XB, Xue M, Zou HX, Liu YS, Ungar G. Twist-bend nematic phase in biphenylethane-based copolyethers. Soft Matter. 2018;14:3003-11.
42. Sreenilayam SP, Panov VP, Vij JK, Shanker G. The N-TB phase in an achiral asymmetrical bent-core liquid crystal terminated with symmetric alkyl chains. Liq Cryst. 2017;44:244-53.
43. Longa L, Tomczyk W. Twist-bend nematic phase in the presence of molecular chirality. Liq Cryst. 2018;45:2074-85.
44. Greco C, Luckhurst GR, Ferrarini A. Molecular geometry, twist-bend nematic phase and unconventional elasticity: a generalised Maier-Saupe theory. Soft Matter. 2014;10:9318-23.
45. Xiang J, Li YN, Li Q, Paterson DA, Storey JMD, Imrie CT, Lavrentovich OD. Electrically Tunable Selective Reflection of Light from Ultraviolet to Visible and Infrared by Heliconical Cholesterics. Adv Mater. 2015;27:3014-8.
46. Xiang J, Varanytsia A, Minkowski F, Paterson DA, Storey JMD, Imrie CT, Lavrentovich OD, Palffy-Muhoray P. Electrically tunable laser based on oblique heliconical cholesteric liquid crystal. Proc Natl Acad Sci U S A. 2016;113:12925-8.
47. Salili SM, Xiang J, Wang H, Li Q, Paterson DA, Storey JMD, Imrie CT, Lavrentovich OD, Sprunt SN, Gleeson JT, Jakli A. Magnetically tunable selective reflection of light by heliconical cholesterics. Phys Rev E. 2016;94.
48. Abberley JP, Killah R, Walker R, Storey JMD, Imrie CT, Salamonczyk M, Zhu CH, Gorecka E, Pociecha D. Heliconical smectic phases formed by achiral molecules. Nat Commun. 2018;9:228.
49. Salamonczyk M, Vaupotic N, Pociecha D, Walker R, Storey JMD, Imrie CT, Wang C, Zhu CH, Gorecka E. Multi-level chirality in liquid crystals formed by achiral molecules. Nat Commun. 2019;10:1922.
50. Walker R, Pociecha D, Strachan G, Storey JMD, Gorecka E, Imrie CT. Molecular curvature, specific intermolecular interactions and the twist-bend nematic phase: the synthesis and

characterisation of the 1-(4-cyanobiphenyl-4′-yl)-6-(4-alkylanilinebenzylidene-4′-oxy)hexanes (CB6O.m). Soft Matter. 2019;15:3188-97.
51. Frisch MJ, et al. Gaussian 09 (Revision B.01). Wallingford CT: Gaussian Inc.; 2010.
52. Tarini M, Cignoni P, Montani C. Ambient Occlusion and Edge Cueing for Enhancing Real Time Molecular Visualization IEEE Trans Visualization and Computer Graphics. 2006;12:1237-44.
53. Dennington R, Keith T, Millam J. Gauss View, Version 5. Shawnee Mission, KS: Semichem Inc; 2009.
54. Attard GS, Garnett S, Hickman CG, Imrie CT, Taylor L. Asymmetric dimeric liquid-crystals with charge-transfer groups. Liq Cryst. 1990;7:495-508.
55. Henderson PA, Seddon JM, Imrie CT. Methylene- and ether-linked liquid crystal dimers II. Effects of mesogenic linking unit and terminal chain length. Liq Cryst. 2005;32:1499-513.
56. Date RW, Imrie CT, Luckhurst GR, Seddon JM. Smectogenic dimeric liquid-crystals - the preparation and properties of the alpha,omega-bis(4-normal-alkylanilinebenzylidine-4'-oxy)alkanes. Liq Cryst. 1992;12:203-38.
57. Imrie CT, Taylor L. The preparation and properties of low molar mass liquid-crystals possessing lateral alkyl chains. Liq Cryst. 1989;6:1-10.
58. Paterson DA, Xiang J, Singh G, Walker R, Agra-Kooijman DM, Martinez-Felipe A, Gan M, Storey JMD, Kumar S, Lavrentovich OD, Imrie CT. Reversible Isothermal Twist-Bend Nematic-Nematic Phase Transition Driven by the Photoisomerization of an Azobenzene-Based Nonsymmetric Liquid Crystal Dinner. J Am Chem Soc. 2016;138:5283-9.
59. Blatch AE, Luckhurst GR. The liquid crystal properties of symmetric and non-symmetric dimers based on the azobenzene mesogenic group. Liq Cryst. 2000;27:775-87.
60. Attard GS, Date RW, Imrie CT, Luckhurst GR, Roskilly SJ, Seddon JM, Taylor L. Nonsymmetrical dimeric liquid-crystals - the preparation and properties of the alpha-(4-cyanobiphenyl-4'-yloxy)-omega-(4-n-alkylanilinebenzylidene-4'-o xy)alkanes. Liq Cryst. 1994;16:529-81.
61. Imrie CT. Non-symmetric liquid crystal dimers: How to make molecules intercalate. Liq Cryst. 2006;33:1449-54.
62. Donaldson T, Staesche H, Lu ZB, Henderson PA, Achard MF, Imrie CT. Symmetric and non-symmetric chiral liquid crystal dimers. Liq Cryst. 2010;37:1097-110.
63. Craig AA, Imrie CT. Effect of spacer length on the thermal-properties of side-chain liquid-crystal poly(methacrylate)s. J Mater Chem. 1994;4:1705-14.
64. Henderson PA, Cook AG, Imrie CT. Oligomeric liquid crystals: From monomers to trimers. Liq Cryst. 2004;31:1427-34.
65. Dunmur DA. The magic of cyanobiphenyls: celebrity molecules. Liq Cryst. 2015;42:678-87.

66. Cestari M, Frezza E, Ferrarini A, Luckhurst GR. Crucial role of molecular curvature for the bend elastic and flexoelectric properties of liquid crystals: mesogenic dimers as a case study. J Mater Chem. 2011;21:12303-8.
67. Hogan JL, Imrie CT, Luckhurst GR. Asymmetric dimeric liquid-crystals - the preparation and properties of the alpha-(4-cyanobiphenyl-4'-oxy)-omega-(4-normal-alkylanilinebenzylidene-4 '-oxy)hexanes. Liq Cryst. 1988;3:645-50.
68. Imrie CT, Henderson PA, Seddon JM. Non-symmetric liquid crystal trimers. The first example of a triply-intercalated alternating smectic C phase. J Mater Chem. 2004;14:2486-8.
69. Blatch AE, Fletcher ID, Luckhurst GR. The intercalated smectic-a phase - the liquid-crystal properties of the alpha(4-cyanobiphenyl-4'-yloxy)-omega-(4-alkyloxycinnamoate)alkanes. Liq Cryst. 1995;18:801-9.
70. Henderson PA, Niemeyer O, Imrie CT. Methylene-linked liquid crystal dimers. Liq Cryst. 2001;28:463-72.
71. Chan TN, Lu ZB, Yam WS, Yeap GY, Imrie CT. Non-symmetric liquid crystal dimers containing an isoflavone moiety. Liq Cryst. 2012;39:393-402.
72. Lee HC, Lu ZB, Henderson PA, Achard MF, Mahmood WAK, Yeap GY, Imrie CT. Cholesteryl-based liquid crystal dimers containing a sulfur-sulfur link in the flexible spacer. Liq Cryst. 2012;39:259-68.
73. Yeap GY, Hng TC, Yeap SY, Gorecka E, Ito MM, Ueno K, Okamoto M, Mahmood WAK, Imrie CT. Why do non-symmetric dimers intercalate? The synthesis and characterisation of the -(4-benzylidene-substituted-aniline-4'-oxy)--(2-methylbutyl-4'-(4''-phen yl)benzoateoxy)alkanes. Liq Cryst. 2009;36:1431-41.